Astron. Astrophys. 331, 661–668 (1998)

ASTRONOMY AND ASTROPHYSICS

A multifrequency study of G182.4+4.3: a new supernova remnant in the Galactic anti-centre

R. Kothes, E. Fürst, and W. Reich

Max-Planck-Institut für Radioastronomie, Auf dem Hügel 69, D-53121 Bonn, Germany

Received 30 April 1997 / Accepted 16 October 1997

Abstract. A new supernova remnant (G182.4+4.3) in the Galactic anti-centre region has been detected at radio frequencies. Observations at 1400 MHz, 2675 MHz, 4850 MHz, and at 10450 MHz with the Effelsberg 100-m telescope reveal a shell structure of about 50' across. The flux density radio spectral index is $\alpha = -0.42 \pm 0.10$, ($S_\nu \propto \nu^\alpha$). The polarization percentage of the brighter part of the shell is about 40%. At 4850 MHz the polarization percentage near the peak of the shell exceeds 60%. The Faraday rotation measure varies between 0 rad m^{-2} and 70 rad m^{-2}. The total flux density extrapolated to 1 GHz is 1.24 ± 0.38 Jy leading to a radio surface brightness of $\Sigma_{1\ GHz} = 7.5\ 10^{-23}$ Watt m^{-2} Hz^{-1} sr^{-1}. HI line observations of neutral hydrogen show that the column density towards G182.4+4.3 must be $\leq 4\ 10^{21}$ cm^{-2}. No X-ray emission is visible in the ROSAT all-sky survey at the position of the new supernova remnant. This corresponds to an upper limit of 6.2 10^{-2} counts s^{-1}. Some information on the nature of G182.4+4.3 is obtained from a discussion of these observations: G182.4+4.3 is at a distance of ≥ 3 kpc and probably expanding according to the classical Sedov equations. Assuming an initial explosion energy of 10^{51} erg the following parameters are obtained: $n_0 \approx 0.013$ cm^{-3}, a radius of $R \approx 22.5$ pc, a swept-up mass of $M_{sw} \approx 14$ M$_\odot$, $kT \approx 5.0$ keV, $age = 3800$ years, and $V_{exp} = 2300$ km s^{-1}.

Key words: ISM: individual objects: G182.4+4.3 – ISM: supernova remnants – polarization – radio continuum: ISM

1. Introduction

The population of supernova remnants (SNRs) is known to be lowest in the direction of the anti-centre of the Galaxy: The number density of stars is lower than towards the central region of the Galaxy as is the average number density of the interstellar gas. Hence, supernova explosions are rare. Because of the low mass of the interstellar gas with which the star fragments interact, the surface brightness of their remnants is rather low. In the past, many of such objects remained undetected. In the course of followup observations of the Galactic plane survey at 2695 MHz (Reich et al. 1984,1990a; Fürst et al. 1990) and at 1400 MHz (Reich et al. 1990b, 1997) we looked at various positions and detected some 30 previously unknown SNRs (Reich et al., 1988). Another new SNR (G182.4+4.3) was recently detected in the anti-centre region at a frequency of 4850 MHz. We made additional observations of G182.4+4.3 with the Effelsberg 100-m telescope at 1400 MHz, 2675 MHz and 10450 MHz to allow a detailed analysis of the spectral and polarization behaviour and the investigation of some physical parameters. Neutral hydrogen observations have been made to obtain the HI column density towards the new SNR.

Send offprint requests to: R. Kothes

2. Radio continuum observations

All radio continuum observations were made with receivers equipped with cooled HEMT amplifiers. Some important parameters are summarized in Table 1.

All observations except those at 1400 MHz have been made in the equatorial coordinate system. At 2675 MHz the telescope was moved in orthogonal directions, at the two other frequencies the scan direction was along the azimuth. At 1400 MHz the scans were made along Galactic longitude and latitude. The standard data reduction has been applied, which is based on the NOD2 format (Haslam, 1974). The multi-feed observations at 4850 MHz and at 10450 MHz were restored using the algorithm described by Emerson et al. (1979) and transformed into the equatorial coordinate system. Baseline improvement by unsharp masking (Sofue and Reich, 1979) and the "PLAIT" algorithm described by Emerson and Gräve (1988) were applied to all observations. The results are shown in Fig. 1 for the total intensity and in Fig. 2 for the polarization. The radio map at 1400 MHz (Fig. 1a) is shown after subtraction of three point-like sources ($\alpha_{B1950} = 6^h4^m45^s$, $\delta_{B1950} = 28°58'$; $\alpha_{B1950} = 6^h6^m19^s$, $\delta_{B1950} = 29°17'$; $\alpha_{B1950} = 6^h7^m17^s$, $\delta_{B1950} = 28°43'$). Fig. 2d shows the projected magnetic field after correction for the Faraday rotation (see Sect. 3).

Table 1. Parameters of the receiver systems and the mapping procedure

Frequency [MHz]	1400	2675	4850	10450
Feeds	1	1	2	4
T_{sys} [K]	30	45	30	50
Bandwidth [MHz]	20	40	500	300
Number of receivers	2	2	4	8
HPBW [']	9.4	4.4	2.5	1.2
Scanning velocity ['/min]	240	120	60	40
Step interval ["]	240	120	60	20
Size ['×']	240×84	100×100	70×70	46×46
Date of observation	Feb./March 1997	Sept./Nov. 1996	July 1996/Jan. 1997	Dec. 1996
Main Calibrator	3C286	3C286	3C286	3C286
Flux density of 3C286 [Jy]	14.4	10.4	7.5	4.5
Linear Polarization of 3C286 [%]	-	9.9	11.3	11.8
Polarization angle for 3C286 [°]	-	33	33	33
Secondary Calibrator	-	3C138	3C138	3C138
Integration time [sec/data point]	1	1	1	0.5
Number of Coverages	3	4	8	9
r.m.s. total intensity [mJy/beam]	10	6	0.5	1.2
r.m.s. polarization [mJy/beam]	-	3	0.2	0.2

The overall structure of the new SNR is best visible at a frequency of 4850 MHz (Fig. 1c): A typical shell with a diameter of about 50'. The shell is most pronounced in the south-west direction. At 2675 MHz this shell is well above the noise, while at 1400 MHz it suffers from confusion with unrelated background emission. At 10450 MHz only the bright shell was observed. At all frequencies (except at 1400 MHz, where no polarization data have been analysed) the object shows strong linear polarization. This polarization combined with the shell-type nature of the object make the classification as a shell-type SNR reasonable.

3. The analysis of the radio continuum observations

The integrated flux density of the new SNR can only be reliably estimated from the 4850 MHz map (Fig. 1c). After subtracting the 14 stronger compact sources from this map the integration in rings yields a flux density of 620 ± 50 mJy.

Therefore, the estimation of the flux density spectral index is based on the bright south western shell, which is visible at all four frequencies. Integrating the flux density in total power and linear polarization intensity of the shell in concentric rings within a sector of 110° starting at the projected centre of $\alpha_{B1950} = 6^h5^m12^s$, $\delta_{B1950} = 29°2'$ yields Fig. 3. Here all maps, except that at 1400 MHz, have been convolved to a unique beam of 5'.

From these figures the integrated flux density and polarization as well as the polarization percentage have been obtained. The result is listed in Table 2.

The flux density spectrum for the shell is shown in Fig. 4.

The flux density spectral index as derived from Fig. 4 ($\alpha = -0.44 \pm 0.10$, $S_\nu \propto \nu^\alpha$) has been tested by differential spectral index plots (TT-plots, see Turtle et al., 1962). Spectral indices obtained with this method are less dependent on remaining background emission. This method was restricted to the bright shell and only the values averaged over the rings in Fig. 3 were used. The result is plotted in Fig. 5.

Table 2. Results from ring integration of the south western shell

Frequency [MHz]	TP[mJy]	PI[mJy]	%-Pol.
1400	360 ± 75	-	-
2675	250 ± 35	115 ± 13	47 ± 12
4850	203 ± 16	100 ± 7	49 ± 3
10450	146 ± 30	68 ± 12	45 ± 8

Similar values as for the integrated flux density are obtained. A relatively large scatter is found for the TT-plot between 2675 MHz and 10450 MHz (Fig. 5b). A careful investigation shows that in the inner part of the shell, up to a radius of 15', the spectral index seems to be smaller ($\alpha = -0.57 \pm 0.09$) than near a radius of 19' ($\alpha = -0.38 \pm 0.05$). Whether this effect is real or an artifact caused by the uncertain baselevels due to different background fluctuations in the maps remains open (Fig. 1a). Summarizing, the radio flux density spectral index of G182.4+4.3 is well represented by $\alpha = -0.42 \pm 0.10$.

The method of differential plots between total power and linear polarisation was used to derive the percentage polarization without the influence of baselevel effects. Using the values averaged over the 2' wide rings (as used in Fig. 3) the following values are obtained: $38 \pm 9\%$ at 10450 MHz, $49 \pm 4\%$ at 4850 MHz, and $38 \pm 7\%$ at 2675 MHz. Within the errors these values are identical to those obtained from ring integration (see Table 2). The large error at 10450 MHz is caused by distortion of the base level (Fig. 3c).

Using the map at 4850 MHz (the map with the highest signal to noise ratio in total power and linear polarization) at the original angular resolution the variation of the polarization percentage with radius can be obtained. It is displayed in Fig. 6.

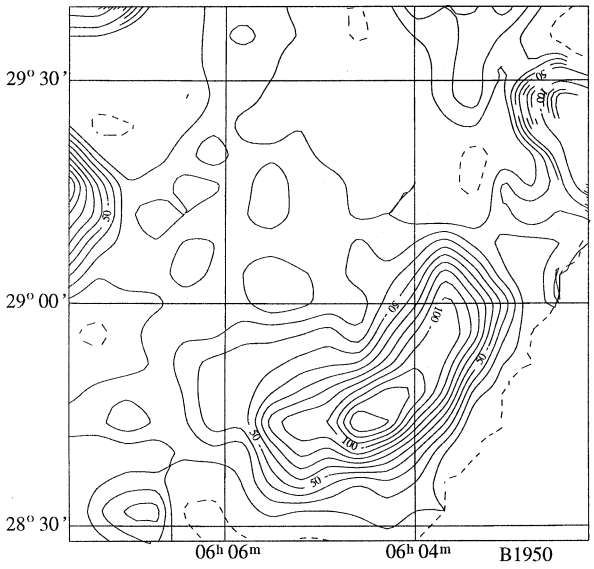

Fig. 1a. Radio map of G182.4+4.3 at 1400 MHz in total intensity after subtraction of point-like sources as listed in Sect. 2. Contours are at 0 mJy/beam (dashed contour), and at 20 to 140 mJy/beam in steps of 10 mJy/beam.

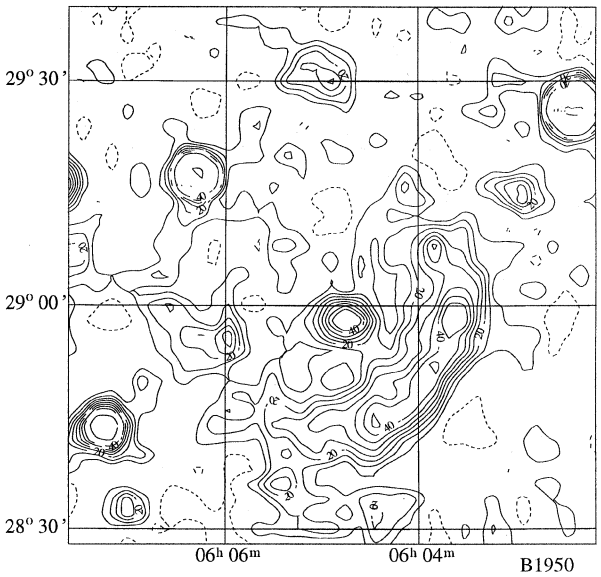

Fig. 1b. Radio map of G182.4+4.3 at 2675 MHz in total intensity. Contours are at 0 (dashed contour), 10, 15, 20, 25, 30, 40, 50, 60, 70, 80, 100, 120, and 140 mJy/beam.

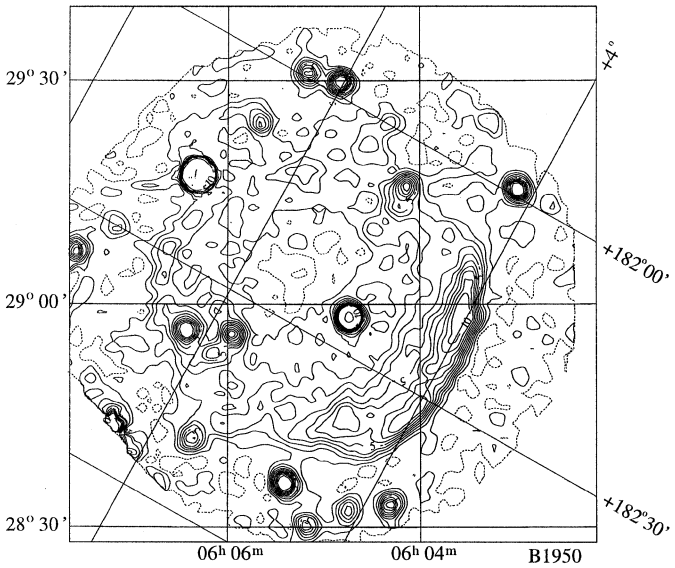

Fig. 1c. Radio map of G182.4+4.3 at 4850 MHz in total intensity. Contours are at 0 mJy/beam (dashed contour), and at 1 to 10 mJy/beam in steps of 1 mJy/beam, and at 20, 30, 40, and 50 mJy/beam.

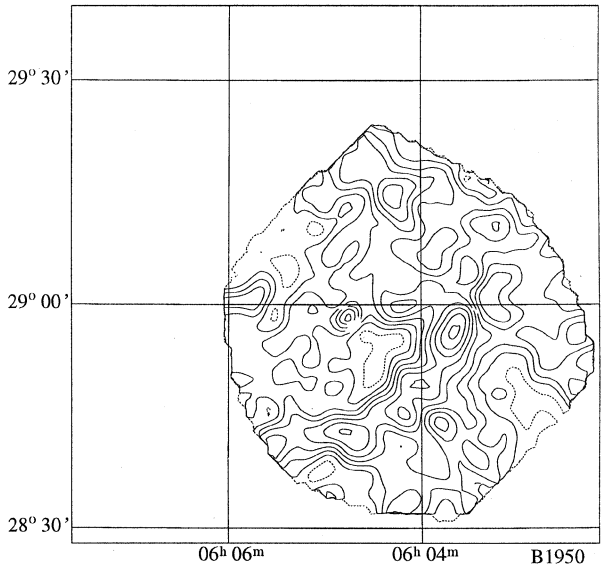

Fig. 1d. Radio map of G182.4+4.3 at 10450 MHz in total intensity. Contours are at 0 mJy/beam (dashed contour), and 2 to 16 mJy/beam in steps of 2 mJy/beam.

Near the peak of the shell the polarization percentage exceeds 60%, while in the inner part it is close to 45%.

The three higher frequencies were used to estimate the Faraday rotation measure. The rotation measure is close to 0 rad m^{-2} for the northern part of the shell and increases towards the middle part to 40 rad m^{-2}. A peak value of 70 rad m^{-2} is obtained near the southern end of the shell. The corrected magnetic field orientation within the shell is shown in Fig. 2d at 4850 MHz.

4. Neutral hydrogen observations

HI line observations do not provide any information on the distance to objects in this part of the Galaxy, but they may be useful for the investigation of evolutionary models. Notably, the knowledge of the total HI column density is shown in Sect. 5 to be of particular interest.

The HI line observations have been made with a two channel cooled HEMT receiver. A 2x512-channel autocorrelator (512 channels for each receiver) was used as backend. The frequency

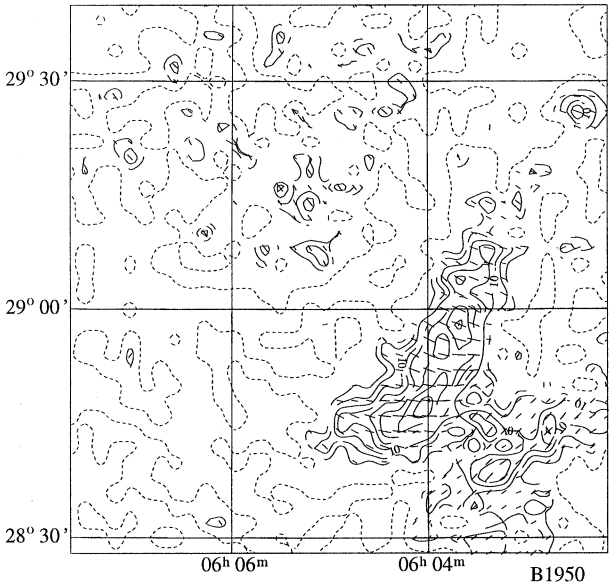

Fig. 2a. Radio map of G182.4+4.3 at 2675 MHz in polarization intensity. Contours are at 0 mJy/beam (dashed contour), and at 6 to 20 mJy/beam in steps of 2 mJy/beam.

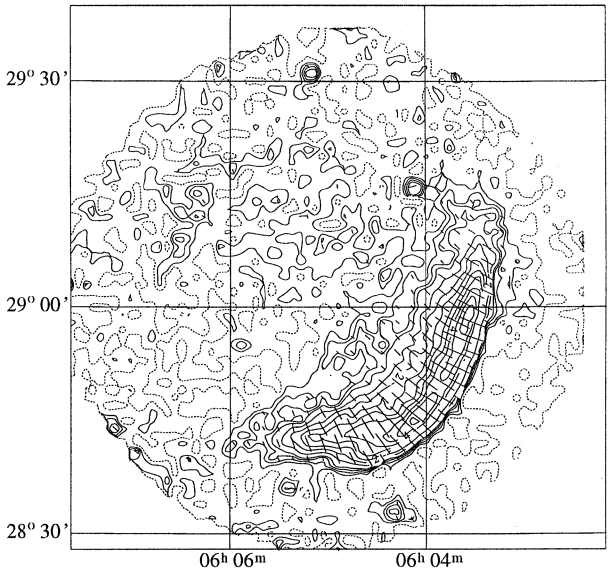

Fig. 2b. Radio map of G182.4+4.3 at 4850 MHz in polarization intensity. Contours are at 0 mJy/beam (dashed contour), 0.4 to 1.0 mJy/beam in steps of 0.2 mJy/beam, and at 1.0 to 5.0 mJy/beam in steps of 0.5 mJy/beam.

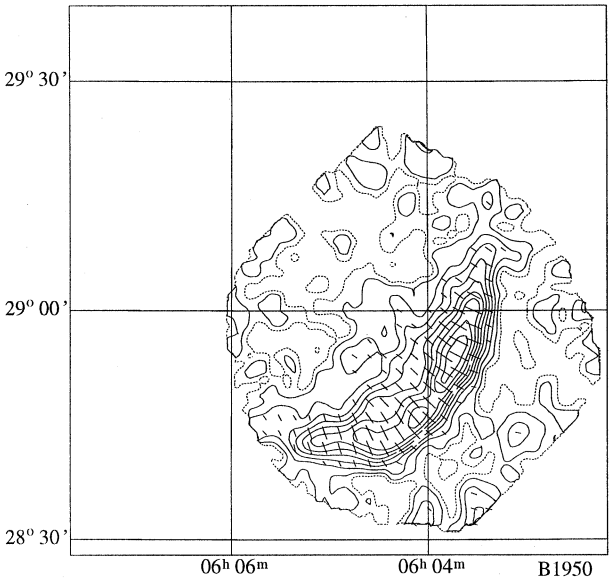

Fig. 2c. Radio map of G182.4+4.3 at 10450 MHz in polarization intensity. Contours are at 0 mJy/beam (dashed contour), 0.5, 1, 1.5, 2, 2.5, 3, 3.5, 4, and 4.5 mJy/beam.

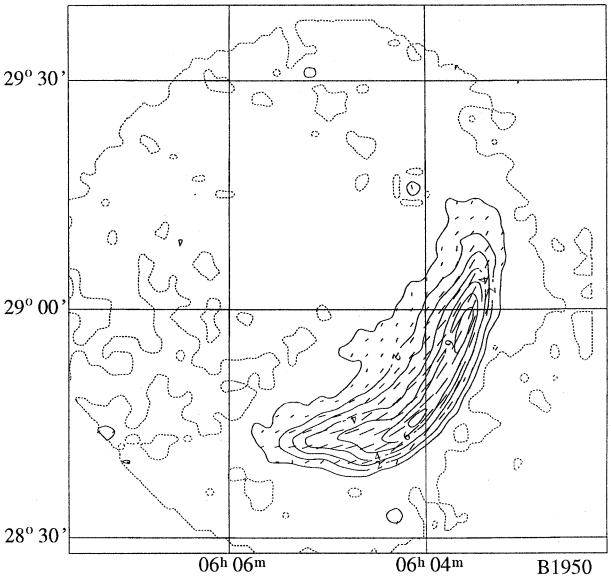

Fig. 2d. The radio shell of G182.4+4.3 at 4850 MHz with the projected magnetic field overlayed. The field is corrected for Faraday rotation (See Sect. 3).

switching technique was used with a signal and reference band separated by 3.5 MHz. The signal band was centered at a velocity of 0 km s^{-1} (LSR). A velocity range of 660 km s^{-1} was covered with a velocity resolution of 1.29 km s^{-1}. The integration time was 30 s. The brightness temperature scale was derived from observations of S7 (l = 132°, b = −1°) (Williams 1973). All profiles were corrected for stray radiation according to the procedure developed by Kalberla et al. (1980). An area of 2.5° × 2.5° was covered at a grid spacing of 9'.

HI column densities have been derived from the brightness temperature $T_B(v)$ according to $\Delta N_H(cm^{-2}) = 1.823\ 10^{18} \int \Delta T_B(v)\, dv$ (Kerr 1968). A map of the HI column density between -200 km s^{-1} and +200 km s^{-1} is shown in Fig. 7. Contours of the total power emission of G182.4+4.3 at 4850 MHz are overlaid.

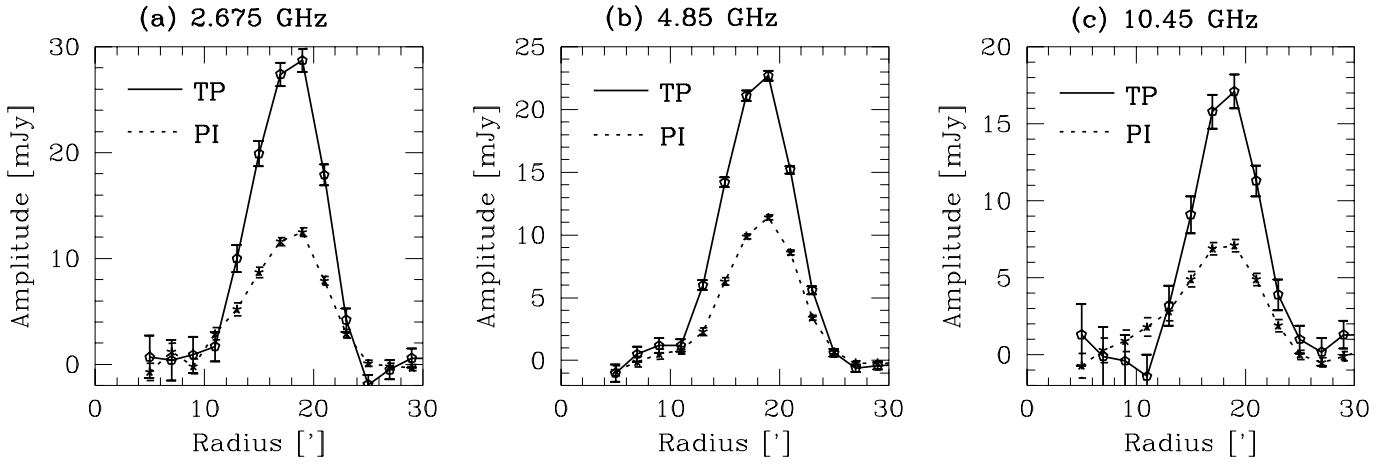

Fig. 3a–c. Integration of the south western shell in rings within a sector of 110° for total power (TP) and polarized intensity (PI). The amplitude denotes the flux density per data point averaged over each ring. The width of each ring is 2'.

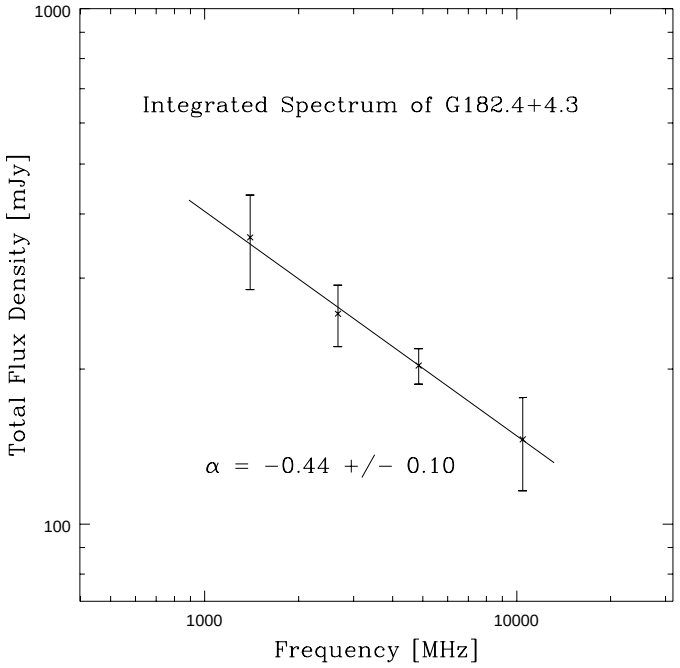

Fig. 4. The radio spectrum of the south western shell of G182.4+4.3 as derived from ring integration.

The column density varies between 3.6 10^{21} cm^{-2} and 4.2 10^{21} cm^{-2} across the SNR. There might be a weak correlation between the HI column density and the SNR total power intensity. However, such a correlation cannot be proved by the current observations. The main result of the HI line observations is that the column density towards G182.4+4.3 must be $\leq$ 4 10^{21} cm^{-2}.

5. Discussion

The radio morphology, the tangential orientation of the magnetic field, and the radio flux density spectrum are those of a classical shell. Extrapolating the spectrum to a frequency of 1 GHz using a flux density spectral index of $\alpha = -0.42$ the flux density is 1.24 ± 0.38 Jy. With a size of Θ = 50' this value transforms into a surface brightness Σ:

$$\Sigma_{1\ GHz}[Watt\ m^{-2}\ Hz^{-1}\ sr^{-1}] = 1.505\ 10^{-19} \frac{S[Jy]}{\Theta^2}$$
$$= 7.5\ 10^{-23}$$

This is the second lowest surface brightness of all known SNRs.

From Fig. 1c the half width of the strong shell can be estimated to about 4', approximately one tenth of the overall size of the remnant. Assuming a sector of 110° of a spherical shell of thickness 4' and a flux density of 410 mJy extrapolated to 1 GHz from the spectrum in Fig. 4 the minimum energy E_{min} (energy in relativistic particles and the magnetic field) as well as the minimum magnetic field strength B_{min} of the bright part of the shell can be derived:

$$E_{min}(erg) = 2.7\ 10^{47}\ d(kpc)^{\frac{17}{7}}$$

$$B_{min}(\mu Gs) = 21\ d(kpc)^{\frac{-2}{7}}$$

The low surface brightness may be used to derive the range of possible values of the ambient interstellar number density n_0. According to an investigation of $\Sigma(n_0)$ by Berkhuijsen (1986) there exists a correlation between Σ and n_0. The scatter in this correlation is very large and it produces a wide range of possible values of n_0:

$$0.001 \leq n_0(cm^{-3}) \leq 0.1$$

A low number density is also favoured by the low Faraday rotation measure RM over a large fraction of the shell. If this value is caused only by internal effects and given the shell thickness, $n_{shell} \approx 4\ n_0$, and $B_{\parallel} \approx B_{min}$ the density is

$$n_0(cm^{-3}) \leq 8.6 \cdot 10^{-4}\ |RM|\ d(kpc)^{-\frac{5}{7}}$$

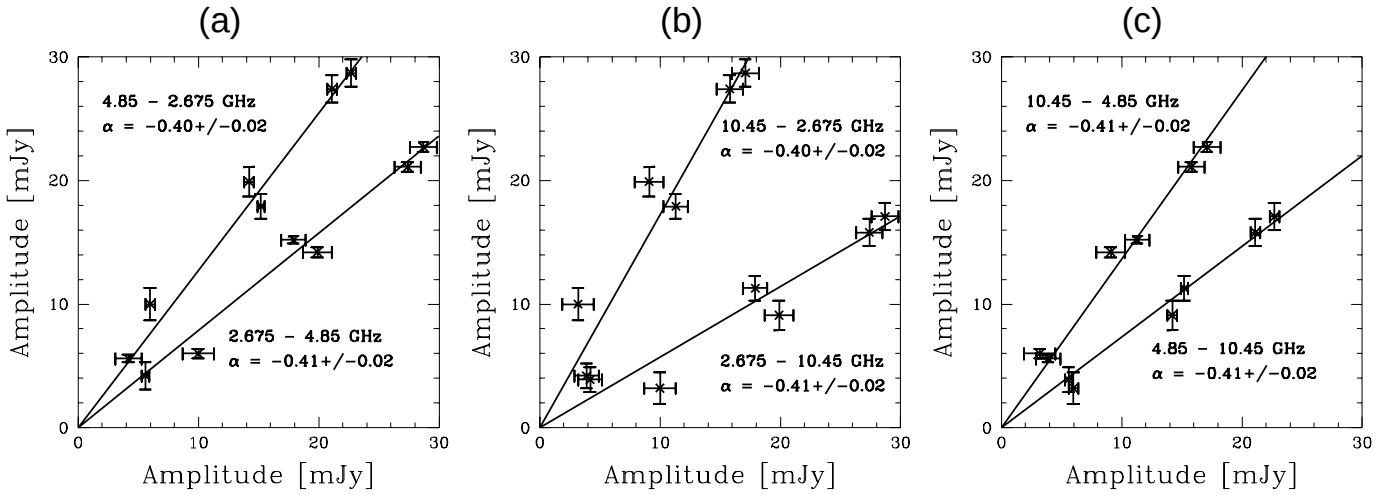

Fig. 5a–c. TT-plot of the bright shell between 2675 MHz and 4850 MHz **a**, 2675 MHz and 10450 MHz **b**, and 4850 MHz and 10450 MHz **c**.

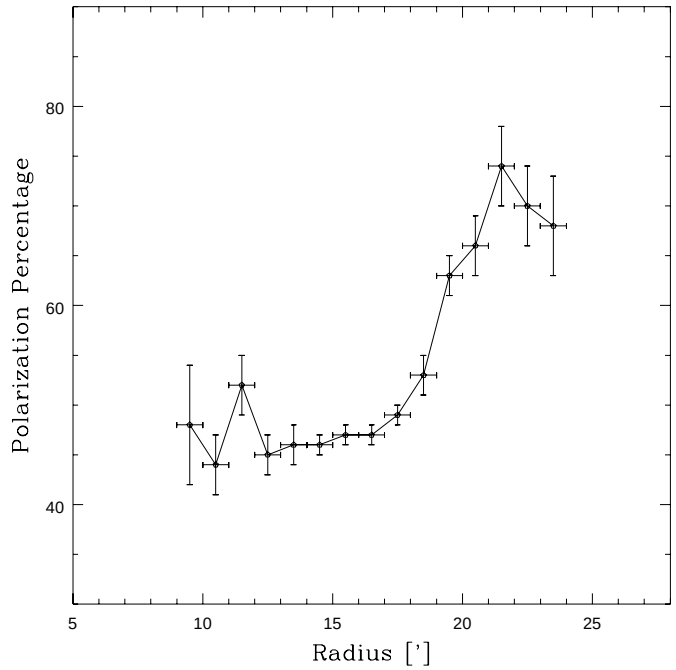

Fig. 6. The variation of the polarization percentage of the shell at 4850 MHz as a function of the radius.

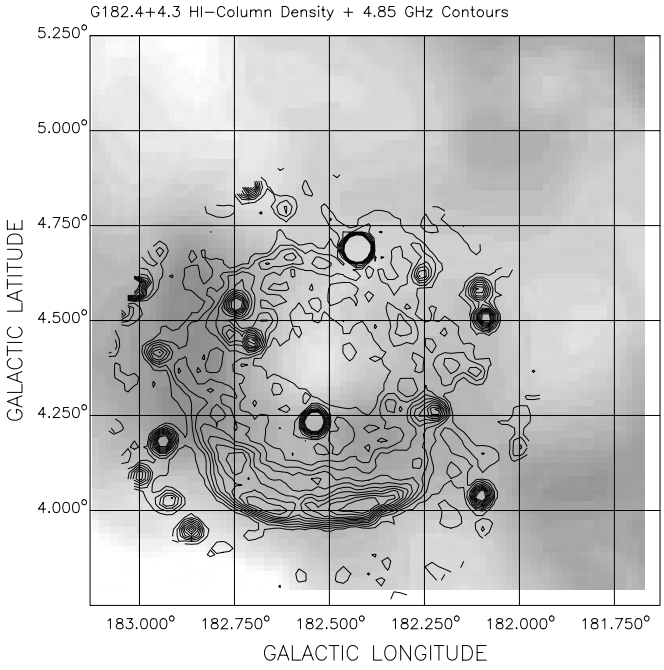

Fig. 7. The HI column density integrated from -200 km s^{-1} to +200 km s^{-1} towards G182.4+4.3. The grey scale levels start from white (3.1 10^{21} cm^{-2} in steps of 0.05 10^{21} cm^{-2}. The peak value is 4.2 10^{21} cm^{-2}. Contours of the total power emission of G182.4+4.3 at 4850 MHz are overlaid.

As found in Sect. 3 the detected Faraday rotation varies systematically from $|RM|$ = 0 rad m^{-2} near the northern end of the shell to about $|RM|$ = 70 rad m^{-2} near the southern end with an average of about $|RM|$ = 40 rad m^{-2}. For the average value the number density is $n_0(cm^{-3}) \leq 0.032\ d(kpc)^{-\frac{5}{7}}$. Some of the Faraday rotation may occur in the interstellar medium: for another SNR only 3.8° away (G179.0+2.7, Fürst & Reich 1985) the Faraday rotation measure through the whole Galaxy was estimated to be $|RM| \leq 15$ rad m^{-2}. The variation of $|RM|$ = 70 rad m^{-2} across the shell suggest internal origin, although a variation of the interstellar rotation of this order over a distance of $\approx$ 30' cannot be excluded. However, even a somewhat larger internal Faraday rotation will result in a low ambient number density. For a flux density spectral index of $\alpha = -0.42$ the maximum of linear polarization of a synchrotron source is 68%. Since the observed polarization percentage is close to 60% not only the ambient density must be small but also a well ordered magnetic field is required. Using the slab model of Burn (1966) the ratio of the random to uniform magnetic field is ≤ 0.37.

A further estimate of the ambient density of G182.4+4.3 is given by the missing X-ray emission in the ROSAT all-sky

survey. Near G182.4+4.3 this corresponds to an upper limit of 6.2 10^{-2} counts s^{-1} (Aschenbach, 1997, private communication). The count rate may be converted into the upper limit of the unabsorbed X-ray flux density F_{X0max} provided the gas temperature and the absorbing column density N_H are known. The temperature for a classical shell may range between kT=0.1 keV and kT=5.0 keV. The peak HI column density towards the direction of G182.4+4.3 is $N_H \approx 4\ 10^{21}\mathrm{cm}^{-2}$ but smaller values are possible if the SNR is rather local. The resulting X-ray luminosity L_X in the ROSAT band (0.1-2.4 keV) is then

$$L_X(10^{33} erg\ s^{-1}) = 0.12\ d^2(kpc)\ F_{X0max}(10^{-12} erg\ cm^{-2}\ s^{-1})$$

The X-ray luminosity of a sphere of Radius R(pc) can be calculated assuming an ambient density $n_0(\mathrm{cm}^{-3})$:

$$L_{Xcal}(erg\ s^{-1}) = 3\ 10^{56}\ R^3(pc)\ n_0^2(cm^{-3})\ P(\Delta E, T)$$

(Heiles, 1964; Tucker, 1971), where $P(\Delta E, T)$ is the emissivity integrated over the energy band ΔE for a temperature T. P has been calculated by Tucker and Koren (1971a,b). Using the radius of G182.4+4.3 (25') yields:

$$L_{Xcal}(10^{33} erg\ s^{-1}) = 1270\ d^3(kpc)\ n_0^2(cm^{-3})\ P(10^{-23})$$

Comparing both values an upper limit for the ambient density is obtained:

$$n_0(cm^{-3}) \leq 0.01\ d^{-\frac{1}{2}}(kpc) \times \left(\frac{F_{X0max}\left(10^{-12} erg\ cm^{-2}\ s^{-1}\right)}{P\left(10^{-23}\right)} \right)^{\frac{1}{2}}$$

The mean value of $\sqrt{\frac{F_{X0max}}{P}}$ is ≈ 1.5 for N_H column densities between $10^{20}\mathrm{cm}^{-2}$ and $4\ 10^{21}\mathrm{cm}^{-2}$ and a temperature interval between kT = 0.3 keV and kT = 5.0 keV, the variation being within a factor 2. For a temperature as low as kT = 0.1 keV the value is 0.4 and 10.0 for the lower and upper column density respectively.

Independent of the distance to G182.4+4.3 the ambient number density is rather low ($n_0 < 0.02$ cm^{-3}).

Some information on the distance can be obtained from the ambient density and the morphology of the SNR. The shell morphology, the flux density spectral index, and the tangential magnetic field classify G182.4+4.3 as a SNR well beyond the free expansion hydrodynamic phase, probably in the Sedov type of expansion. This phase requires a ratio $\eta = M_{swept-up}/M_{ejected} \gg 1$ (Woltjer 1972). Given the ambient density as derived from the X-ray emission the swept-up mass for a radius of 25' (R(pc)=7.5 d(kpc)) is:

$$M_{swept-up}(M_\odot) \leq 0.37\ d^{\frac{5}{2}} \left(\frac{F_{X0max}}{P} \right)^{\frac{1}{2}}$$

The investigation of the X-ray spectrum of two young shell-type SNRs (SN1006 and Tycho's SNR) by Hamilton et al.(1986a,1986b) shows that they probably have mass ratios of 2.4 and 0.9, respectively. But according to their X-ray spectrum these remnants cannot be explained by a pure Sedov expansion. Hamilton et al. conclude that the radio emission of these remnants has perhaps to be attributed to the ejecta, which would be in agreement with the observed radial magnetic field. The tangential magnetic field of G182.4+4.3 indicates that this SNR is dominated by the blast wave with a much larger mass ratio η. A ratio of $\eta = 1$ ($M_{swept-up} = 1.4\ M_\odot$) gives a very lower limit of the distance of $d = 1.6\ kpc$. However, a mass ratio of $\eta = 5 - 10$ seems much more reasonable, indicating that $d \geq 3$ kpc. At a distance of 3 kpc and a Galactic longitude of $l \approx 180°$ the z-height of the maximum density of the HI gas layer is between 0 and 100 pc above the Galactic plane defined by $b = 0°$ (Burton 1988). The latitude of the SNR results in a z-height ≥ 230 pc. For a distance of 3 kpc and using the classical equations describing the Sedov type of expansion and an initial explosion energy of 10^{51}erg the following parameters are obtained: $n_0 \approx 0.013$ cm^{-3}, a swept-up mass of $M_{sw} \approx 14$ M$_\odot$, $kT \approx 5.0$ keV, $age = 3800$ years, and $V_{exp} = 2300$ km s^{-1}. The radius of the source at 3 kpc distance is 22.5 pc, not unusual for evolved SNRs. This distance places G182.4+4.3 in front of the outer spiral arm III. However, a larger distance cannot be excluded from the above investigation.

If the new SNR is compared with the SNR G156.2+5.7, which was detected by Pfeffermann et al. (1991) by its strong X-ray emission, it can be noted that both SNRs show the same very low radio surface brightness (Reich et al., 1992), but are very different in X-rays. What might be the reason for this? According to White and Long (1991) the X-ray luminosity may increase if the supernova shell evaporates interstellar clouds. If C is the ratio between the mass of the clouds and the mass of the intercloud medium and if τ is the ratio between the evaporation time of the clouds and the age of the SNR, the luminosity varies as:

$$L_X = L_X^{Sedov} \cdot \left(1 + \frac{C}{1+\tau}\right)^2$$

The different X-ray luminosity of G182.4+4.3 and G156.2+5.7 may be caused by a different mass ratio C. A difference of 10 in C may increase the luminosity by a factor 100. G182.4+4.3 probably expands into a medium with low density and a low fraction of clouds.

6. Summary

The radio source G182.4+4.3 has been identified as a SNR with very low radio surface brightness. The radio observations classify the source as a shell-type SNR expanding into an ambient medium of low number density. The source is probably in the so-called Sedov-type expansion. The low ambient density favours a location in the interarm region either in front or behind the Perseus arm. A low density is supported by the probable high z-height of the remnant of ≥ 230 pc. G182.4+4.3 is most likely the remnant of a Typ Ia supernova explosion.

Acknowledgements. We like to thank B. Uyaniker for his help with the HI-line observations and reduction. We also thank Dr. B. Aschenbach for the prompt information on the upper limit of the X-ray emission of G182.4+4.3 from the ROSAT all-sky survey. We kindly acknowledge the assistance of the technical teams at Effelsberg and Bonn.

References

Berkhuijsen E.M.: 1986, A&A 166, 257
Burn P.J.: 1966, MNRAS 133, 67
Burton W.B.: 1988, In: Galactic and Extragalactic Radio Astromony, p347, G.L. Verschuur and K.I. Kellermann (eds), Springer Verlag
Emerson D.T., Klein U., Haslam C.G.T.: 1979, A&A 76, 92
Emerson D.T., Gräve R.: 1988, A&A 190, 353
Fürst E., Reich W.: 1985, A&A 154, 377
Fürst E., Reich W., Reich P., Reif K.: 1990, A&AS 85, 691
Hamilton A.J.S., Sarazin C.L., Szymkowiak A.E.:1986a, ApJ 300, 698
Hamilton A.J.S., Sarazin C.L., Szymkowiak A.E.:1986b, ApJ 300, 713
Haslam C.G.T.: 1974, A&AS 15, 333
Heiles C.: 1964, ApJ 140, 470
Kalberla P.M.W., Mebold U., Reich W.: 1980, A&A 82, 275
Kerr F.J.: 1968, In: Nebulae and Interstellar Matter, Stars and Stellar Systems Vol.III, p575, B.M. Middlekorst and L.H. Aller (eds)
Pfeffermann E., Aschenbach B., Predehl P.: 1991, A&A 246, L28
Reich W., Fürst E., Steffen P., Reif K., Haslam C.G.T.: 1984, A&AS 58, 197
Reich W., Fürst E., Reich P., Junkes N.: 1988 In: Roger R.S., Landecker T.L. (eds) Proc. IAU Col. 101, Supernova Remnants and the Interstellar Medium, Cambridge University Press, p.293
Reich W., Fürst E., Reich P., Reif K.: 1990a, A&AS 85, 633
Reich W., Reich P., Fürst E.: 1990b, A&AS 83, 539
Reich W., Fürst E., Arnal E.M.: 1992, A&A 256, 214
Reich P., Reich W., Fürst E.:1997, A&AS in press
Sofue Y., Reich W.: 1979, A&AS 38, 251
Tucker W.H.: 1971, Science 172, 372
Tucker W.H., Koren M.: 1971a, ApJ 168, 283
Tucker W.H., Koren M.: 1971b, ApJ 170, 621
Turtle A.J., Pugh J.F., Kenderline S., Pauliny-Toth I.I.K.: 1962, MNRAS 124, 297
White R.L., Long K.S.: 1991, ApJ 373, 543
Williams D.R.W.: 1973, A&AS 8, 505
Woltjer L.: 1972, ARA&A 10, 129

This article was processed by the author using Springer-Verlag LaTeX A&A style file *L-AA* version 3.